

Aerodynamic prediction of helicopter rotor in forward flight using blade element theory

M.F. Yaakub^{1*}, A.A. Wahab¹, A. Abdullah¹, N.A.R. Nik Mohd² and S.S. Shamsuddin¹

¹Department of Aeronautical Engineering,
Faculty of Mechanical and Manufacturing Engineering,
Universiti Tun Hussein Onn Malaysia,
86400 Batu Pahat, Johor, Malaysia.

*Email: fauziy@uthm.edu.my

Phone: +6074533395 Fax: +6074536080

²Department of Aeronautics, Automotive and Ocean Engineering,
Faculty of Mechanical Engineering,
Universiti Teknologi Malaysia,
81310, Skudai, Malaysia.

ABSTRACT

In this study, the helicopter blade in forward-flight condition was investigated. The blade element theory (BET) was used throughout this analysis to investigate the angle of attack variations at the blade cross sections, lift distribution along the blade and effects of increasing helicopter speed. Prouty's helicopter data was used to validate the analysis results. In this analysis, the helicopter blade was divided into 50 equally spaced elements and the azimuth ψ was set at 7.2° for each movement of the blade. The helicopter speed of 80 m/s was considered. The analysis revealed that the computation results were in good agreement with Prouty's diagram. Furthermore, it was also evident that in the case of a helicopter in forward-flight condition, the blade at retreating side was generally at low angle of attack and experienced low lift, in contrast to the blade at advancing side. The increment of the helicopter speed affected the lift distribution along the blade. The reverse flow area was widened two times from that given by the original Prouty's diagram. In addition, it was proven that each helicopter has its own speed limit called velocity never exceed (VNE). It was also shown that BET is important in conducting the analysis to modify the helicopter blade design for the aerodynamic characteristics' improvement as well as stability and general performance enhancement for the helicopter.

Keywords: Aerodynamics, blade element theory, rotor, forward flight

INTRODUCTION

The helicopter is a unique flying vehicle designed to perform various manoeuvring flights such as hovering, forward, rearward, sideward, and vertical translations. These capabilities make helicopter a viable and extensively used vehicle platform in missions such as air patrol, search and rescue (SAR), transportation to rural places or offshore platform in which the take-off and landing space is often limited. For a traditional helicopter configuration, the main rotor is the key component that produces lift and propulsive forces. The tail rotor generates a thrust force to counteract the fuselage torque

arising from the rotation of the main rotor and is mainly used for the directional (yaw) motion control of the helicopter. During the flight, the main rotor spins at a constant rotational speed. The change in the collective and cyclic pitch angles input by the pilot will alter the aerodynamic loads of the rotor; hence, changing the translation motion of the helicopter. In hover flight, the main rotor experiences equivalent collective and cyclic pitch inputs to stay afloat in equilibrium. However, in a forward-flight manoeuvre, the forward speed causes the rotor to experience high and low airspeed regions at both sides of the rotor which complicates analysis compared to a hovering flight [1-4].

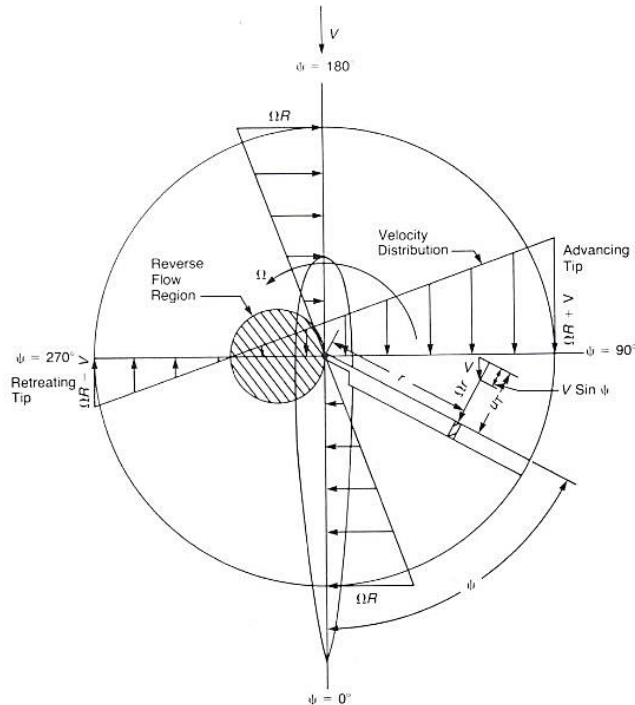


Figure 1. Velocity distribution of the helicopter blade in forward flight [4].

However, the current speed of the helicopter is still considered slower than the fixed-wing aircraft. One of the key factors that limit the helicopter capability to achieve faster forward speed is the retreating blade stall. The retreating blade stall condition is a dangerous flight condition in helicopters, where a rotor blade with smaller resultant relative wind will stall after exceeding the critical angle of attack. The lift generation between advancing and retreating side of the blade is different from each other during forward flight where the advancing side experiences significant lift increase compared to the retreating side [1-4]. This is illustrated in Figure 1 which shows that the advancing side encounters increased velocity due to a combination of rotational velocity of the rotor and helicopter's forward speed while the retreating side experiences a decreased velocity. To overcome the dissymmetrical of lift problem in forward flight, the pilot has to control the blade cyclic pitch input to the main rotor blade in order to control both sides of the angle of attack [1-4]. The angle of attack at retreating side must be increased due to its lower relative velocity, while at the advancing side, the blade must operate at a lower angle of attack due to the higher velocity profile. If the retreating side of the angle of attack become too large, then the blade will stall which results in a loss of overall lift from the rotor, which subsequently restricting the forward speed of the helicopter [5-8].

Various recent research activities focused on overcoming the speed limitation imposed by retreating blade stall condition to drive the helicopter at a faster speed beyond its speed limit, Velocity Never Exceed (VNE). The blade planform modification [9-11] is one of the commonly used methods to improve the forward speed of a helicopter. This modification is focused on the design at the tip of the blade whereby a poor design will contribute to serious implication on the rotor performance. The British experimental rotor program (BERP) blade is the most successful design [12, 13] in the blade planform modification which was fitted at GKN-Westland Super Lynx and attained the world speed record of 400.87 km/h for conventional helicopter [14]. Another commonly used method to achieve higher forward speed is to delay flow separation at the retreating blade. This feature can be achieved through the use of passive or active flow control devices installed on the blade. The passive control methods delay the flow separation in the retreating region through the blade geometrical modification and are always in operation, regardless of need or performance penalty. Passive control devices such as Pulse Vortex Generator Jets (PVGJs) [15-17], Direct Synthetic Jet (DSJ) [18, 19], Rod Vortex Generator (RVG) [20] and Vortex Trap Concept [21-23] were designed to generate vortices to reduce flow separation of the retreating blade at a high angle of attack. On the other hand, the second method controls flow by adding energy or momentum to the flow in a regulated manner. Actuators are at the heart of active flow control implementation and several concepts were introduced in literature such as Spar85Def10 concept [24], Active Camber Deformation [25], Variable Droop Leading Edge (VDLE) [26, 27], Nose-Droop Concept [28], Static Extended Trailing Edge (SETE) [29], Trailing-Edge Flap (TEF) [30], and Gurney Flap (GF) [31, 32]. The important step before modifying the standard blade design with the installation of the passive or active devices on the helicopter blade is to determine the exact location of flow separation region along the retreating side [1-4]. The focus of this paper is to explore the implementation of BET for predicting the aerodynamic performance for the helicopter blade during the forward-flight condition; hence, determining the exact location of flow separation region from BET analysis. Several forward speeds were considered for this analysis to investigate the effect of increasing forward speed on flow separation region.

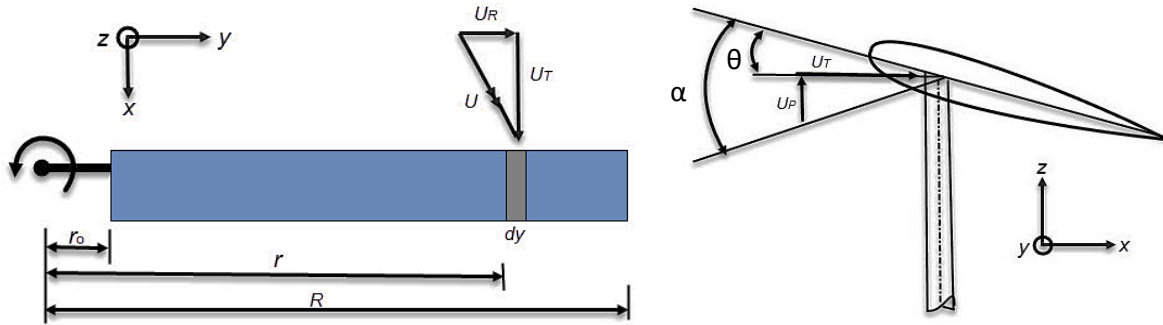
METHODS AND MATERIALS

Theoretical Background

There are several methods that can be used to analyse the aerodynamic characteristics of helicopter blade such as the momentum theory, blade element theory (BET), and vortex method [1-4]. Among the above-mentioned methods, BET is widely used to provide a fast prediction of the rotor aerodynamics forces such as rotor thrust, lift and drag coefficients, induced velocity, and rotor disk loading at each element along the blade either in the advancing or retreating side. Additionally, dynamic coefficients such as the lateral and longitudinal flapping coefficients, pitching, sectional blade angle of attack, collective pitch, and rotor coning angles acting on the blade also can be obtained using BET [1-4]. Other advantages of BET are that the method is relatively simple for predicting the performance of a rotor and the results of the analysis are reasonably accurate.

In this paper, BET was used throughout the analysis. In BET, each blade section was assumed to act as a quasi-2D aerofoil to produce aerodynamic forces. Figure 2 shows the velocity components and angle of attack that occur at the blade element on the helicopter blade. In forward flight, a function of the radial station, r and the azimuth

position, ψ was used to analyse the angle of attack and increment of lift at the element. Furthermore, the blade flapping motion, blade feathering motion, and velocity of the blade were also taken into account in this analysis to obtain the angle of attack at the various elements of the blade.



(a) Velocity components at blade element (b) Angle of attack at blade element

Figure 2. Aerodynamic environment at a typical blade element [1-4].

The angle of attack along the blade radial and azimuth position is shown in Eq. (1).

$$\alpha_r = \theta + \tan^{-1}\left(\frac{U_P}{U_T}\right) \quad (1)$$

where U_T is the tangential velocity (Equation 2), U_P is the perpendicular velocity (Equation 3), and θ is blade pitch. The calculation of tangential and perpendicular velocity is given as follows:

$$U_T(r, \psi) = \Omega r + \mu \Omega R \sin \psi \quad (2)$$

$$U_P(r, \psi) = (V \alpha_s - v) - r \frac{\partial \beta}{\partial t} - \mu \Omega R \beta \cos \psi \quad (3)$$

$$U_R(r, \psi) = V \cos \psi + (V \alpha_s - v) \beta \quad (4)$$

where $V \alpha_s$ is the component of forward speed parallel to the rotor shaft and local induced velocity, v is used for this analysis is shown in Equations 5 and 6, respectively.

$$v = v_1 \left(1 + \frac{r}{R} \cos \psi\right) \quad (5)$$

$$v_1 = \frac{\Omega R C_T}{\mu} \frac{1}{2} \quad (6)$$

The helicopter blade pitch (or feathering) motion $\theta(r, \psi)$ and blade flapping as the function of blade azimuth $\beta(\psi)$ can be described as the Fourier series in Equations 7 and 8 respectively [2, 6].

$$\theta(r, \psi) = \theta_0 + \frac{r}{R} \theta_{nv} - A_1 \cos \psi - B_1 \sin \psi \quad (7)$$

$$\beta(\psi) = a_0 - \sum_{n=1}^{\infty} (a_{n_s} \cos n\psi - b_{n_s} \sin n\psi) \tag{8}$$

where θ_0 is collective pitch, θ_{tw} is twist angle, A_l is lateral cyclic, B_l is longitudinal cyclic, a_o is the rotor coning angle, a_{ns} is longitudinal flapping and lateral flapping is b_{ns} . The angle of attack along the blade radial and azimuth position is simplified in Equation 9 [6]

$$\alpha_r = \frac{1}{\frac{r}{R} + \mu \sin \psi} \left\{ \begin{array}{l} \frac{r}{R} \left[\theta_0 + \theta_1 \frac{r}{R} - (A_1 - b_{1s}) \cos \psi - (B_1 + a_{1s}) \sin \psi \right] - \frac{v}{\Omega R} \left(1 + \frac{r}{R} \cos \psi \right) \\ + \mu \left[\alpha_{TTP} + \left(\theta_0 + \theta_1 \frac{r}{R} \right) \sin \psi - a_0 \cos \psi - (A_1 - b_{1s}) \sin \psi \cos \psi \right. \\ \left. - (B_1 + a_{1s}) \sin^2 \psi \right] \end{array} \right\} \tag{9}$$

The increment of lift on each blade element along the blade and around the azimuth is computed by using Equation 10.

$$\frac{\Delta L}{\Delta r} = \frac{1}{2} \rho U_T^2 a \alpha_r c \tag{10}$$

where ρ is density, a is the slope of aerofoil lift curve per radian and c is the blade chord.

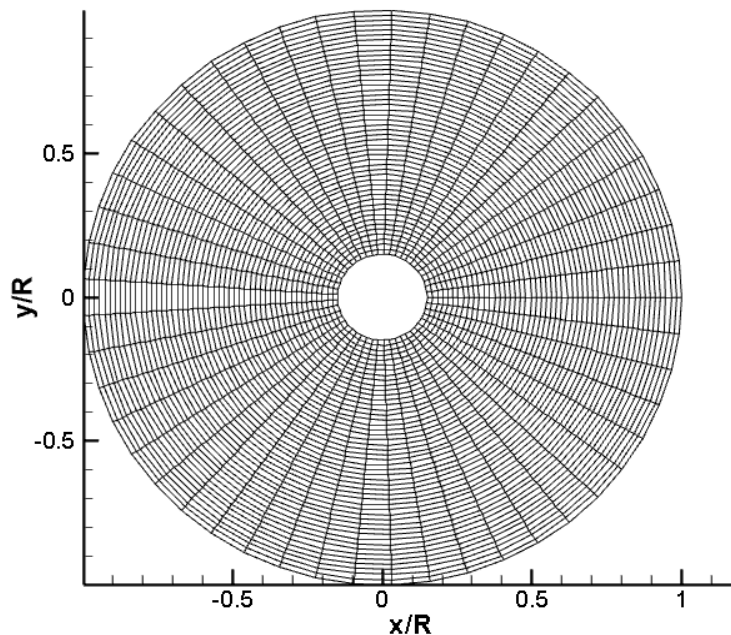


Figure 3. Meshing of the blade movement area (rotor blade is divided into 50 elements along the span of the blade with equally spaced azimuth angle spacing ($\psi = 7.2^\circ$ each)).

Blade Data and Parameter

In BET, the angle of attack and lift on the entire blade is the integration of the angle of attack and lift on all the blade elements from the centre of the rotor to the tip. The rotor

blade from Prouty's example helicopter [4] was used in the analysis, whereby the blade was divided into 50 equally spaced elements and azimuth range, ψ at 7.2° for each movement of the blade (Figure 3). The analysis of this paper was based on the data from Prouty's example helicopter given in Table 1.

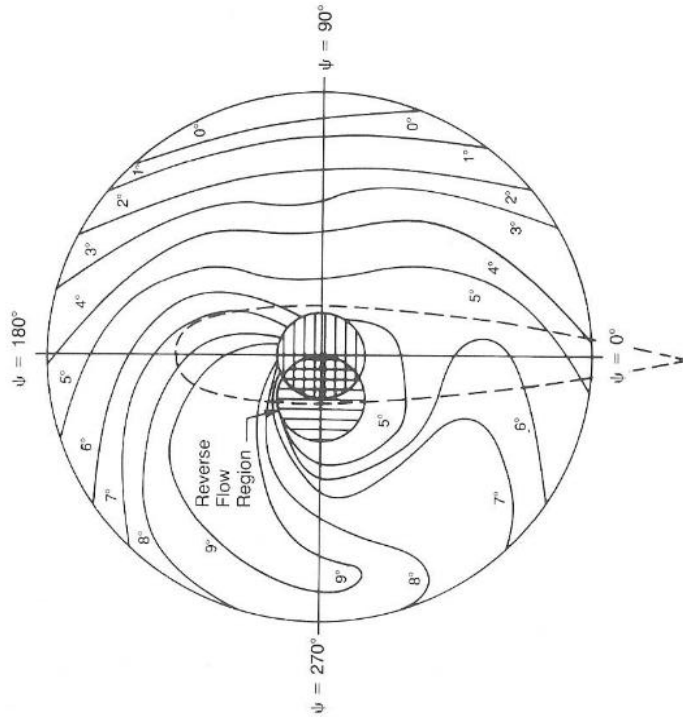
Table 1. Blade parameter and Prouty's data used for analysis.

Blade Parameter	
No. of blade	2
Blade radial section	50
Blade azimuth section	7.2°
Sample Data [4]	
Aerofoil	NACA 0012
Blade radius, R	9.144 m
Chord, c	0.61 m
Blade cutout ratio, r_0	0.15
Tip speed, ΩR	197 m/s
Speed, V	59.16 m/s
Tip speed ratio, μ	0.3
Collective pitch, θ_0	15.8°
Lateral cyclic, A_I	-2.3°
Longitudinal cyclic, B_I	4.9°
Coning angle, a_0	4.3°
Angle of tip path plane, a_{TPP}	-3.7°
Twist angle, θ_{tw}	-10°

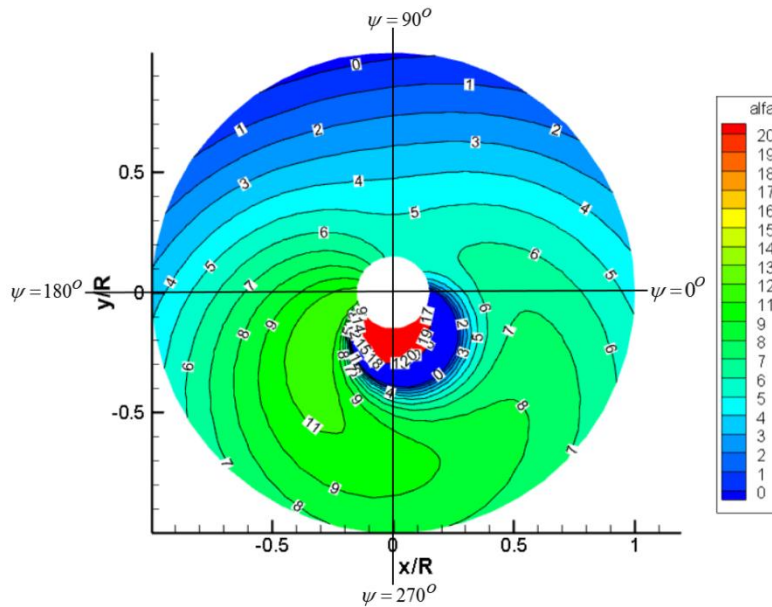
RESULTS AND DISCUSSION

In this study, the analysis was done based on the data obtained from Prouty's research on helicopters. In order to ensure that the analysis was done properly and accurately, the computed distribution of the angle of attack along the helicopter main rotor blade in forward-flight condition was compared with the established findings from Prouty's analysis [4]. The result of that analysis as illustrated in Figure 4 showed that the computed analysis was in good agreement with the Prouty's diagram. From Figure 4(b), the analysis gave evidence that the advancing side region ($y/R > 0$) contained a low angle of attack while at retreating side ($y/R < 0$ regions), the analysis produced a high angle of attack and a reverse flow area. Reverse flow area is an area with no lift and indicates that the airflow moved across the trailing edge toward the leading edge of the blade [1-4]. The reverse flow area can also be identified by observing rotation area with a significantly high angle of attack value.

To investigate the lift forces produced along the blade at advancing and retreating sides, the movement of the blade rotation in 1-2-3 position sequence (counter clockwise) was considered as shown in Figure 5. The analysis considered three azimuth angles at $\psi = 43.2^\circ / \psi = 223.2^\circ$, $\psi = 93.6^\circ / \psi = 273.6^\circ$ and $\psi = 136.8^\circ / \psi = 316.8^\circ$. The data from Figure 4(b) and the lift coefficient for NACA0012 at difference Mach numbers from Paul [33] were used in this analysis in order to obtain the lift distribution along Blades A and B.



(a) The angle of attack distribution from Prouty's analysis at $V=60\text{m/s}$ [4].



(b) Computed analysis

Figure 4. Angle of attack and reverse flow area comparison (a) Prouty's diagram (b) The computed analysis.

Figure 6 shows the angle of attack and lift distribution along Blades A and B at positions 1, 2, and 3. From Figure 6(a), the general trend for all azimuth angles showed that a high angle of attack occurred at the retreating side (Blade A) compared with advancing side (Blade B). The azimuth $\psi = 223.2^\circ$ (Position 1) of Blade A contained the highest angle of attack, which was about 11.3° located at the 37% of Blade A from the hub of the rotor. Meanwhile, for Blade B $\psi = 43.2^\circ$ (position 1), the highest angle of

attack was around 6.3° . Positions 2 and 3 had the similar curve of the angle of attack compared to Position 1. The negative angle of attack at inboard of the Blade A at the retreating side was the reverse flow area where the angle of attack value increased at the inboard of the blade from $r/R=0.2$ (Position 1) to $r/R=0.4$ (Position 3). At the advancing side (Blade B at azimuth $\psi = 43.2^\circ$, $\psi=93.6^\circ$ and $\psi = 136.8^\circ$) in Figure 6(a), the high angle of attack occurred at inboard of the blade and it gradually decreased from root to tip of the blade. This reduction was due to the blade twist effect [1-4]. From this analysis, the retreating side having the critical area contained the high angle of attack at the $0.65R$ and $1.0R$, which was the suitable location to place the separation control device.

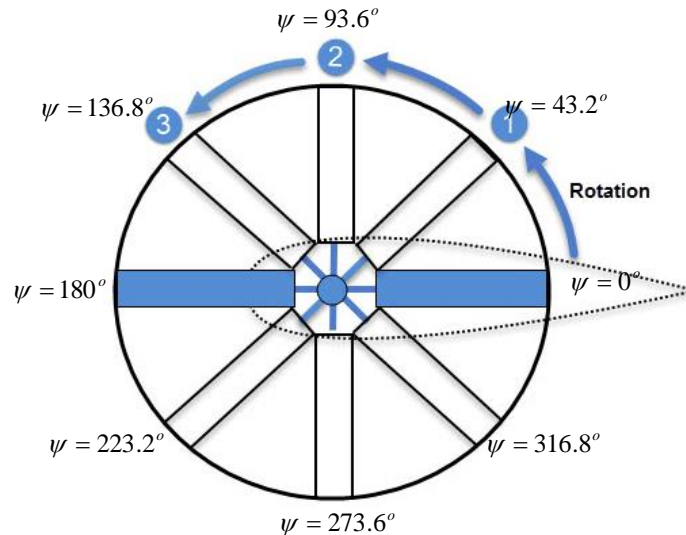


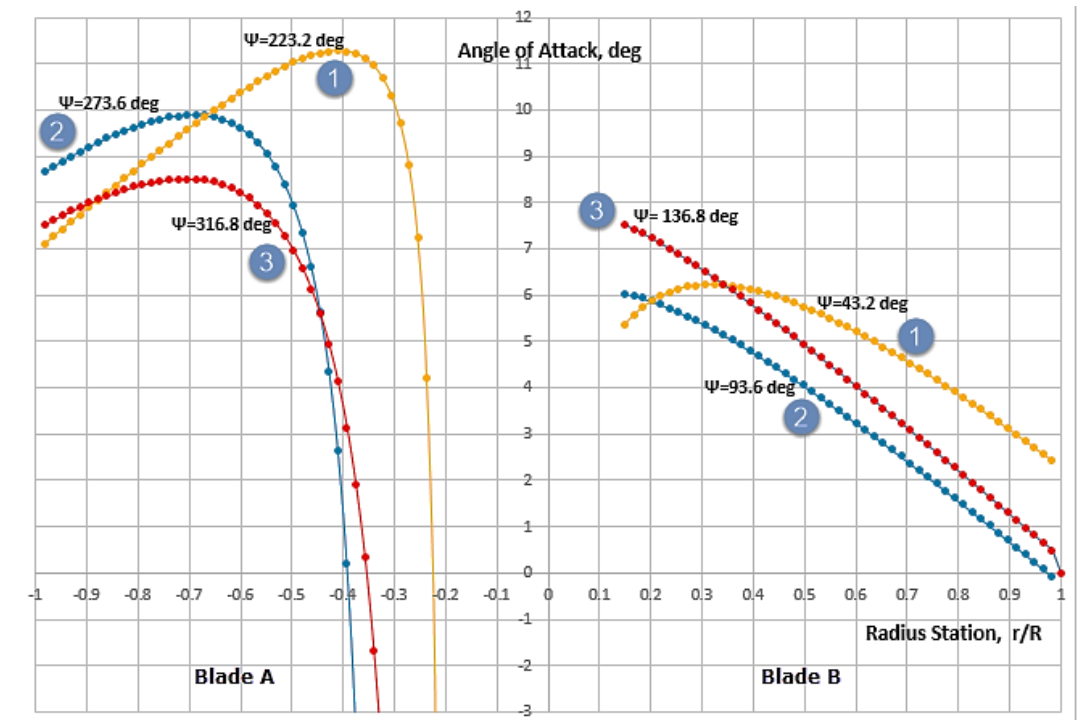
Figure 5. Rotation of main rotor blade.

Table 2. Lift per running meter at advancing and retreating side.

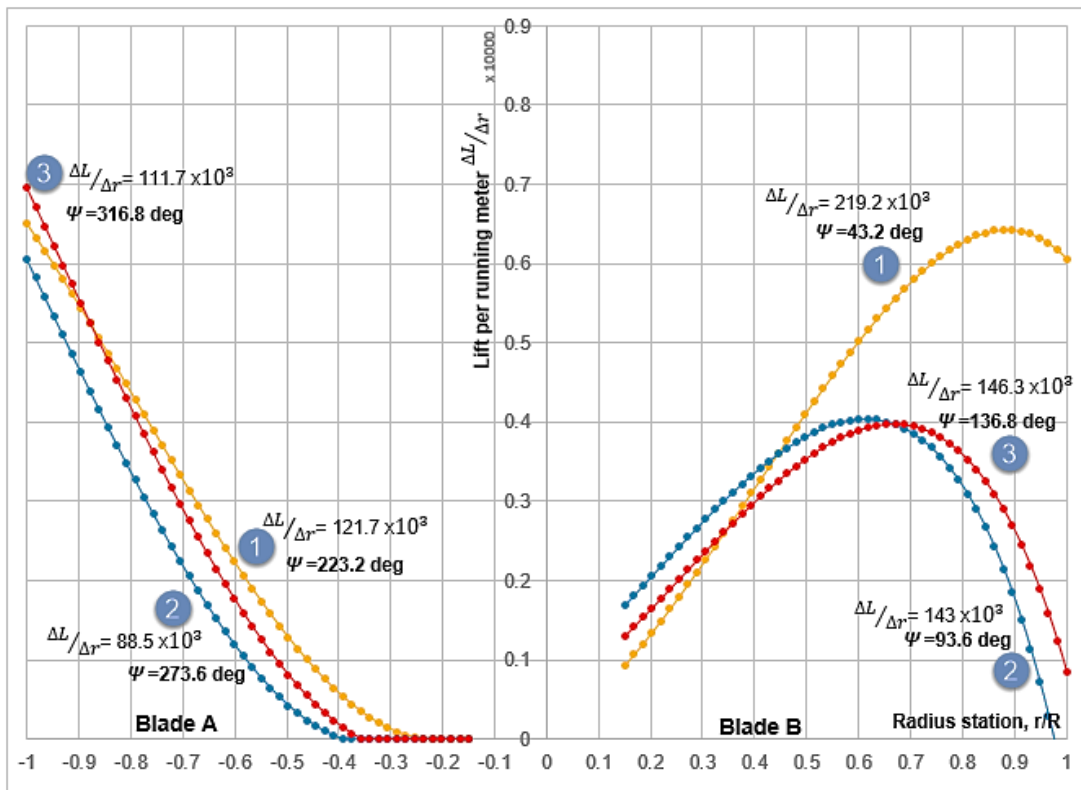
Position	Retreating side, Blade A		Advancing side Blade B	
	Azimuth, ψ	Lift per running meter, $\Delta L / \Delta r$	Azimuth, ψ	Lift per running meter, $\Delta L / \Delta r$
1	223.2°	121.7×10^3	43.2°	219.2×10^3
2	273.6°	88.5×10^3	93.6°	143.0×10^3
3	316.8°	111.7×10^3	136.8°	146.3×10^3

Figure 6(b) is plotted based on the data from Figure 6(a) to show the lift distribution at Blades A and B. Table 2 shows the lift at advancing and retreating blade for Positions 1 to 3. From Figure 6(b) and Table 2 for the triple positions of rotation, the advancing blade side had an additional lift ($\Delta L / \Delta r$) compared to the retreating blade side. The lower lift value at the retreating blade was due to the reverse flow region where no lift forces were generated from the rotor hub to $0.4R$. The dissymmetrical of lift affected the helicopter's forward motion where the helicopter has the tendency to roll to the left at the retreating side. To overcome the extra lift at advancing side, the pilot has to control the helicopter blade manually using cyclic pitch input in order to stabilise the blade by reducing the angle of attack at the retreating side and avoid the unwanted rolling motion to the retreating blade side [1-4]. The result also gives the indication that any installation

of flow control device should focus on the area along the retreating blade from 0.4R to the tip of the blade, 1.0R.



(a)



(b)

Figure 6. Angle of attack and lift distribution for Blades A and B (a) Angle of attack distribution (b) Lift distribution.

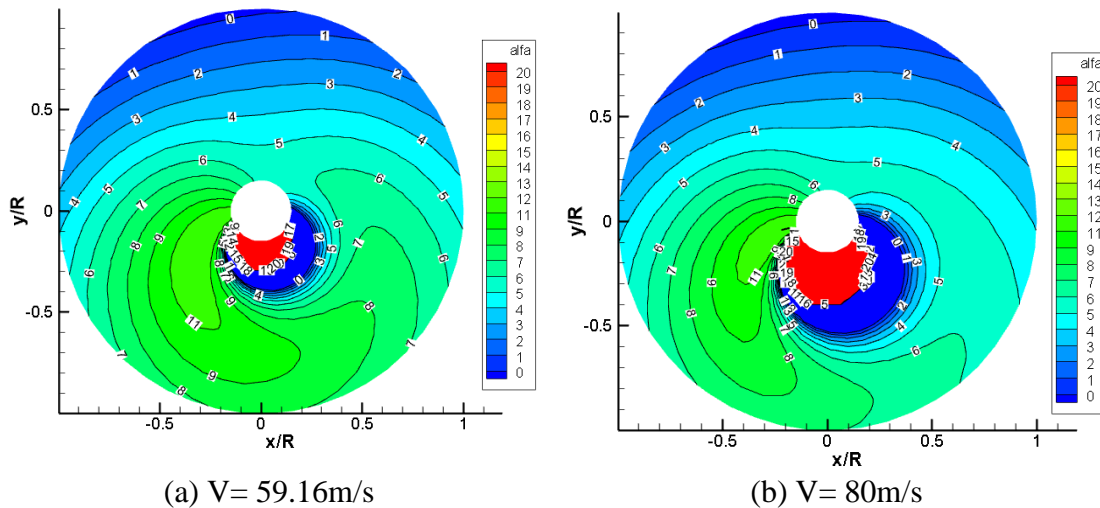


Figure 7. Comparison of the distribution of the angle of attack of the blade for forward speed at $V=60\text{m/s}$ and $V=80\text{m/s}$.

The effect of increasing the helicopter speed is important to understand its limitations, VNE. In this study, the helicopter speed at 80m/s was chosen to compare with Prouty's speed (59.16 m/s) to investigate the aerodynamic characteristic of increasing helicopter speed. Figure 7 shows the distribution of the angle of attack when the helicopter speed increased about 33.33% from $V = 60\text{ m/s}$. From Figure 7, the diameter of reverse flow area at retreating side for $V = 80\text{ m/s}$ increased two times of reverse flow (no lift) region diameter for $V = 60\text{ m/s}$. The distribution of the angle of attack differed for each speed due to the increased speed of the helicopter. This indicated that the lift for the retreating side of the rotor decreased when the speed of the helicopter increased. To ensure safety, every helicopter normally has its limit of speed, VNE (Velocity Never Exceed) to avoid the build-up of reverse flow area and significant low lift at the retreating blade. This factor is a very important indicator to researchers in order to improve the blade aerodynamic performance and also the overall helicopter performance.

CONCLUSIONS

In this paper, the result of the angle of attack and lift distribution along the main rotor blade when the helicopter is in forward-flight condition obtained using BET was presented. The Prouty's example of helicopter data was validated to ensure the angle of attack and lift distribution along the blade was done properly and accurately. Good agreement of angle of attack between BET data and angle of attack diagram was achieved. Based on the findings, the high angle of attack occurred at the advancing side of the rotor starting from the inboard position of the blade and gradually decreased from root to tip of the blade. Meanwhile, the highest angle of attack and reverse flow area occurred at the retreating side. Thus, the results show that the lift of retreating side was lower compared to the advancing side, hence causing the helicopter to roll to the retreating side. Increasing the helicopter speed effect the angle of attack and lift distribution along the blade. The reverse flow area region also increased as the helicopter moved at a faster speed. It can be concluded that aerodynamic parameter based on BET is an important tool for a researcher in analysing helicopter blade in forward-flight condition before modification

of the blade is made. Further studies are recommended on the effect of changing the cyclic pitch of the blade.

ACKNOWLEDGMENTS

The author would like to acknowledge the Malaysia Ministry of the Higher Education, the Ministry of Science, Technology, and Innovation and Universiti Tun Hussein Onn Malaysia for the financial support of this research under the Ph.D. scholarship scheme and Science Fund research grant (Vot. S028).

REFERENCES

- [1] Leishman GJ. Principle of Helicopter Aerodynamic: Cambridge University Press; 2006.
- [2] Gessow A MG. Aerodynamic of Helicopter. New York: Frederick Ungar Publishing Co; 1999.
- [3] W. J. Helicopter Theory: Dover Publications, Inc; 1994.
- [4] RW. P. Helicopter Performance of Stability and Control. PWS Engineering Boston; 2005.
- [5] McCormick D, Anderson T, Wake B, Mac Martin D. Rotorcraft Retreating Blade Stall Control. AIAA; 2000.
- [6] Raghav V, Komerath N. An exploration of radial flow on a rotating blade in retreating blade stall. Journal of the American Helicopter Society. 2013;58:1-10.
- [7] Hooper W. Technology for advanced helicopter. SAE Paper No872370. 1987.
- [8] Gustafson F, Gessow A. Effect of Blade Stalling on the Efficiency of a Helicopter Rotor as Measured in Flight. NACA Technical Note 1250. 1947.
- [9] NAR NM, Wahab A. Feasibility Study on Improving of Helicopter Forward Flight Speed via Modification of the Blade Dimension and Engine Performance. Proceeding of RIVET06. Kuala Lumpur; 2006.
- [10] McVeigh MA, McHugh FJ. Influence of tip shape, chord, blade number, and airfoil on advanced rotor performance. Journal of the American Helicopter Society. 1982;29:55-62.
- [11] Vu NA, Lee JW, Shu JI. Aerodynamic design optimization of helicopter rotor blades including airfoil shape for hover performance. Chinese Journal of Aeronautics. 2013;26:1-8.
- [12] Harrison R, Stacey S, Hansford B. BERP IV: The design development and testing of an advanced rotor blade. 64th Annual Forum of the American Helicopter Society' 2008.
- [13] Brocklehurst A, Beedy J, Barakos G, Badcock K, Richards B. Experimental and CFD investigation of helicopter BERP tip aerodynamics. Integrating CFD and Experiments in Aerodynamics International Symposium. Glasgow; 2007.
- [14] Perry FJ. Aerodynamics of the World Speed Record. 3rd Annual National Forum of the American Helicopter Society. 1987.
- [15] Kostas J, Foucaut J, Stanislas M. The flow produced by pulsed-jet vortex generators in a turbulent boundary layer in an adverse pressure gradient. Flow, Turbulence and Combustion. 2007;78:331-63.
- [16] Godard G, Stanislas M. Control of a decelerating boundary layer. Part 3: Optimization of round jets vortex generators. Aerospace Science Technology. 2006;10:455-64.

- [17] Tilmann CP, Langan KJ, Betterton JG, Wilson MJ. Characterization of pulsed vortex generator jets for active flow control. Land vehicle and sea vehicle (RTO/AVT) symposium. Germany; 2003. p. 51-512.
- [18] McCormick DC, Lozyniak SA, MacMartin DG, Lorber PF. Compact, high-power boundary layer separation control actuation development. Proceeding of ASME Paper No. 18279. 2001.
- [19] Amitay M, Smith DR, Kibens V, Parekh DE, Glezer A. Aerodynamic flow control over an unconventional airfoil using synthetic jet actuators. AIAA Journal. 2001;39:361-70.
- [20] Tejero E, Doerffer P, Szulc O. Application of Passive Control Device on Helicopter Rotor Blades. Journal of the American Helicopter Society. 2016;61:1-13.
- [21] De Gregorio F, Fraioli G. Flow control on a high thickness airfoil by a trapped vortex cavity. 14th Int Sym On Application of Laser Techniques to Fluid Mechanics. Lisbon, Portugal; 2008. p. 143-9.
- [22] Bouferrouk A, Chernyshenko S. Stabilisation of a trapped vortex for enhancing aerodynamic flows. In: 15th Australian Fluid Mechanics Conferences. University of Sydney; 2004.
- [23] Donelli RS IP, Iuliano E, Rosa DD. Optimization on thick airfoil to trap vortices. Report of VortexCell2050. 2008.
- [24] Kerho M. Adaptive airfoil dynamic stall control. Journal of Aircraft. 2007;44:1350-60.
- [25] Kumar D, Cesnik CE. Performance Enhancement in Dynamic Stall Condition Using Active Camber Deformation. Journal of the American Helicopter Society. 2015;60:1-12.
- [26] Chandrasekhara M, Martin PB, Tung C. Compressible Dynamic Stall Control Using a Variable Droop Leading Edge Airfoil. Journal of Aircraft. 2004;41:862-9.
- [27] Qureshi H, Hamdani HR, Parvez K. Effects on dynamic stall on cambered airfoil with drooping leading edge control. 44th AIAA Aerospace Science Meeting and Exhibition; 2006.
- [28] Geissler W, Trenker M. Numerical investigation of dynamic stall control by a nose-drooping device. American Helicopter Society Aerodynamics, Acoustics Test and Evaluation Technical Specialist Meeting; 2002.
- [29] Liu T, Montefort J, Liou W, Pantula S, Shams QA. Lift enhancement by static extended trailing edge. Journal of Aircraft. 2007;44:1939-47.
- [30] Maughmer M, Lesieutre G, Kinzel M. Miniature Trailing-Edge Effectors for Rotorcraft Performance Enhancement. American Helicopter Society 61st Annual Forum. 2007;52:146-58.
- [31] Bae ES, Gandhi F, Maughmer M. Optimally scheduled deployment of gurney flap for rotorcraft power reduction. American Helicopter Society 65th Annual Forum. 2009.
- [32] Gibertini G, Zanotti A, Droandi G, Auteri F, Crosta G. Experimental investigation of a helicopter rotor with Gurney flaps. The Aeronautical Journal. 2017;121:191-212.
- [33] Paul J.C. "Lift and Profile-Drag Characteristic of an Airfoil Section as derived from Measured Helicopter Rotor Hovering Performance". NASA Technical Note 4357. 1958.